

## Ultrafast electron transfer in the recognition of different DNA sequences by a DNA-binding protein with different dynamical conformations

Tanumoy Mondol, Subrata Batabyal and Samir Kumar Pal\*

Department of Chemical, Biological & Macromolecular Sciences, S. N. Bose National Centre for Basic Sciences, Block JD, Sector III, Salt Lake, Kolkata 700 098, India

Communicated by Maxim Frank-Kamenetskii

(Received 23 September 2011; final version received 27 February 2012)

Ultrafast electron transfer (ET) phenomenon in protein and protein–DNA complex is very much crucial and often leads to the regulation of various kinds of redox reactions in biological system. Although, the conformation of the protein in protein–DNA complex is concluded to play the key role in the ET process, till date very little evidences exist in the literature.  $\lambda$ -repressor–operator DNA interaction, particularly  $O_{R1}$  and  $O_{R2}$ , is a key component of the  $\lambda$ -genetic switch and is a model system for understanding the chemical principles of the conformation-dependent ET reaction, governed by differential protein dynamics upon binding with different DNA target sequences. Here, we have explored the photoinduced electron transfer from the tryptophan moieties of the protein  $\lambda$ -repressor to two operators DNA of different sequences ( $O_{R1}$  and  $O_{R2}$ ) using picosecond-resolved fluorescence spectroscopy. The enhanced flexibility and different conformation of the C-terminal domain of the repressor upon complexation with  $O_{R1}$  DNA compared to  $O_{R2}$  DNA are found to have pronounced effect on the rate of ET. We have also observed the ET phenomenon from a dansyl chromophore, bound to the lysine residue, distal from the DNA-binding domain of the protein to the operator DNA with a specific excitation at 299 nm wavelength. The altered ET dynamics as a consequence of differential protein conformation upon specific DNA sequence recognition may have tremendous biological implications.

**Keywords:**  $\lambda$ -repressor; operator DNA; TCSPC; photoinduced electron transfer; different dynamical conformations

### Introduction

Electron transfer (ET) reactions involved in biomacromolecules (DNA and protein) have incredible significance in the various assembly of biological processes including photosynthesis, respiration, enzyme catalysis (Isied, Ogawa, & Wishart, 1992), gene regulation (Augustyn, Merino, & Barton, 2007; Lee, Demple, & Barton, 2009), aging-related molecular disease (Kelley & Barton, 1998), and DNA repair (Wagenknecht, Stemp, & Barton, 1999). The heterocyclic bases are the most reactive moieties of DNA. Removal of a single electron from a heterocyclic base by UV light, ionizing radiation, or chemical oxidation results in the formation of an electron-deficient site or a hole that is guanyl/adenyl radical or cation, which is the product of the exclusion of a single electron from guanine/adenine (Becker & Sevilla, 1993; Butchosa, Simon, & Voityuk, 2010). The hole within DNA is transferred to the guanine (Candeias & Steenken, 1993) moiety as it is the most preferable location available in DNA (Colson, Besler, Close, & Sevilla, 1992). The electron

repair process within DNA generally occurs through ET reaction with active redox species like peptides and proteins. This is due to the presence of amino acids such as tryptophan and tyrosine containing indole and phenol as functional groups respectively in their side chains. The ET phenomenon is undoubtedly governed by the relative orientation and distance of the involved redox species (Butchosa et al., 2010). Consequently, for a protein–DNA complex, the conformation (Chohan et al., 2001; Jones et al., 2002; Ridge et al., 2000; Schulten & Tesch, 1991) of the protein upon complexation with the DNA is extremely crucial for the flow of electron from protein to DNA moiety. In a variety of biological processes, the conformational flexibility of the protein upon DNA binding is the key signal for the propagation of the process further. For example, in a gene regulatory network of bacteriophage  $\lambda$ , different conformational flexibility in the C-terminal domain of the  $\lambda$ -repressor protein upon complexation with two target DNA sites,  $O_{R1}$  and  $O_{R2}$  (Ptashne, 1992), leads to cooperative binding of the protein to the different

\*Corresponding author. Email: skpal@bose.res.in

operator sites, which is vital for the functioning of the genetic switch (Benson, Adams, & Youderian, 1994; Hochschild & Ptashne, 1986). It was widely anticipated that the specificity of this type of complexation depends exclusively on the recognition of the DNA sequence by the protein. However, it can be proposed that thermodynamic factors may take part in the process of recognition which came from the inspection that  $O_{R1}$ - and  $O_{R2}$ -bound repressors have different structures (Deb, Bandyopadhyay, & Roy, 2000). Similarly, recent work with glucocorticoid receptor protein (GRP) suggests that GRP bound to different target sequences has different structures leading to different functional outcomes (Meijsing et al., 2009). The dynamical properties of the protein bound to different target sites are almost obsolete in the existing literature. The present study addresses the key important issues regarding the sequences-dependent binding of the protein to different DNA sites, leading to differential dynamics of the protein in the complexes (Mondol, Batabyal, Mazumder, Roy, & Pal, 2012) and its outcome on the photoinduced electron transfer (PET) dynamics.

In this regard, ET in  $\lambda$ -repressor–DNA complex (Figure 1) is extensively investigated to monitor DNA sequence-dependent change in the protein structure and dynamics after binding with DNA, which can be reflected by the change in the wavelength-dependent fluorescence transients of the intrinsic probe tryptophan in the  $\lambda$ -repressor protein upon complexation with two operators DNA ( $O_{R1}$  and  $O_{R2}$ ) of different sequences, using picosecond-resolved fluorescence spectroscopy. One of the key findings includes similar ET dynamics from dansyl, a widely used extrinsic fluorescent probe, located near the C-terminal region of the protein (Figure 1), to the two operators DNA upon UV excitation.

To confirm the ET reaction, occurring from tryptophan and dansyl to DNA bases, and to rule out the existence of any intramolecular ET between redox-active amino acids inside the protein upon conformational change upon DNA binding, an extensive set of control experiments has been performed with free DNA bases and amino acids in thin films without any interference of solvent or any other biological molecules.

## Materials and methods

The materials and the experimental details are described in the supplementary material.  $\lambda$ -repressor was isolated from a strain of *Escherichia coli* RR1 15  $\Delta$ lac Z carrying a plasmid pEA305 which contains the wild-type *cI* gene under the control of *tac* promoter. The details of the purification procedure have been given in elsewhere (Banik, Saha, Mandal, Bhattacharyya, & Roy, 1992; Saha et al., 1992). Operator DNA sequences,  $O_{R1}$  (5'CGTACCTCTGGCGGTGATAG3') and its comple-

mentary oligonucleotide,  $O_{R2}$  (5'TACAACACGCACGGTGTTAT3') and its complementary oligonucleotide, were purchased from Trilink (USA).

The complexation between dansyl-labeled  $\lambda$ -repressor and ethidium bromide (EtBr)-bound operator DNA was studied within indigenously developed microfluidics setup in stop condition by monitoring the respective change in fluorescence intensity of dansyl as captured by an attached CCD camera in millisecond time resolution (Batabyal, Rakshit, Kar, & Pal, 2012). The specially designed microfluidics chip with the connectors and the syringe pumps (Atlas-ASP011) were from Dolomite, UK and Syrris Ltd., UK, respectively. The Y-shaped microfluidics chip consists of two inlets and a common outlet. The diameter of the microchip was designed to be 440  $\mu$ m. The two inlets were attached to syringe pump by capillary tubes. The capillaries were passed through the shaft of the holder prior to connection with the microfluidics chip. The reagents were propelled using the syringe pump. Fluorescence images were captured in a steady-state flow-stopped condition with a fluorescence microscope (BX-51, Olympus America, Inc.) equipped with a 100-W mercury arc lamp, which was used as excitation source (UV light excitation,  $\lambda_{\text{ex}} = 365$  nm), and a DP72 CCD camera. The excitation light was cut off by using standard filter and the fluorescence was collected through a 10 $\times$  objective. The image processing and analysis were done by 'analySIS' software provided with the microscope. We have selected a small area of interfacial region of the two streams for the analysis purpose. RGB analysis was performed to separate out the blue color from the detected fluorescence. Blue color was chosen as a marker for interaction to avoid out the contribution of EtBr emission, which has negligible blue color in its fluorescence RGB analysis. Therefore, the blue part in the RGB could be accounted solely due to dansylated  $\lambda$ -repressor. The concentration of both dansyl-labeled  $\lambda$ -repressor and operator DNA ( $O_{R1}$ ) was  $2 \times 10^{-6}$  (M) and EtBr concentration was  $8 \times 10^{-6}$  (M). For the system under investigation, the diffusion of the biomolecules with increasing time was monitored. The diffusion coefficient ( $D$ ) was calculated using the following equation for two-dimensional diffusion law (Ozturk, Hassan, & Ugaz, 2010),  $\tau = \frac{d^2}{2D}$ , where ' $d$ ' is the distance travelled by the particle under study in time  $\tau$ . From the obtained diffusion coefficient, the radius of the biological molecule under investigation was estimated using the equation as stated below,  $D = \frac{kT}{6\pi\eta r}$ , where  $k$  is the Boltzmann constant,  $T$  is absolute temperature,  $\eta$  is the viscosity of solvent, and  $r$  is the hydrodynamic radius of the molecule. Our microfluidics approach is found to have immense potentiality for the exploration of diffusion-controlled (Mondol, Batabyal, & Pal, 2012) biophysical studies on the protein as have been done by other techniques (Gomez-Fernandez, Goni, Bach, Restall, & Chapman, 1980; Nada & Terazima, 2003) that are underway in our group.

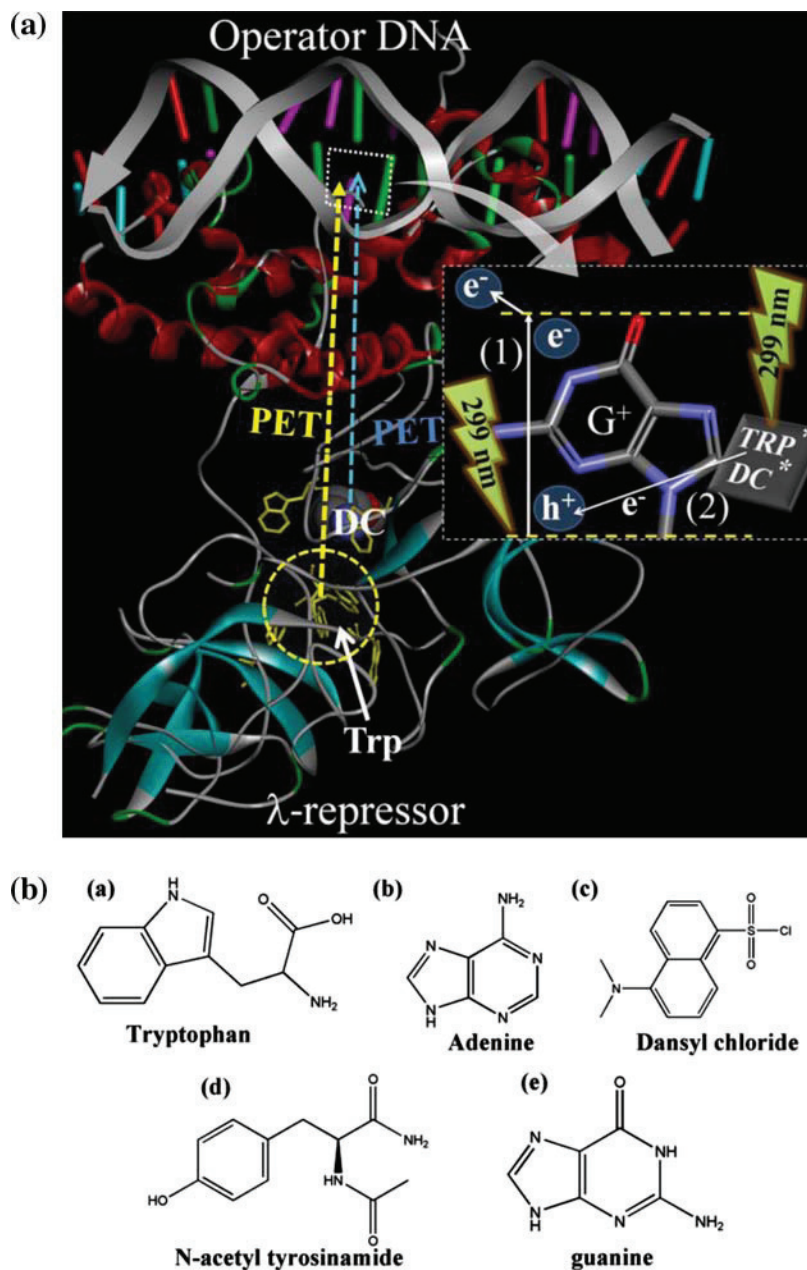


Figure 1. (a) X-ray crystal structure of  $\lambda$ -repressor bound to operator DNA ( $O_{L1}$ ) depicting the simultaneous occurrence of PET from tryptophan and dansyl (bound to lysine in the protein) to guanine radical or cation in the operator DNA is represented schematically. Dotted circle has been drawn to illustrate the major number of tryptophan molecules residing as a cluster near the C-terminal domain. Tryptophan and dansyl are excited at 299 nm. Reaction 1 (1) in the inset shows the removal of electron from guanine (G) forming  $G^+$  (or formation of a hole [ $h^+$ ]) upon 299 nm excitation, and reaction 2 (2) indicates the transfer of electron from excited-state tryptophan and dansyl to  $G^+$ .  $TRP^*$  and  $DC^*$  denote the excited-state tryptophan and dansyl moiety, respectively. (b) Molecular structure of (a) tryptophan, (b) adenine, (c) dansyl chloride, (d) *N*-acetyl tyrosinamide, and (e) guanine.

## Results and discussions

It has to be noted that we have mixed protein and DNA solution with predetermined concentrations and incubated for 1 h for the formation of protein–DNA complex. In order to investigate whether the incubation time is suffi-

cient for the complexation, we have performed Förster resonance energy transfer (FRET) studies within the microfluidics channel as shown in Figure 2(a)–(d). In this regard, we have dansylated the protein (dansyl emission at 515 nm) and labeled the  $O_{R1}$  DNA with EtBr (absorption at 510 nm). Details of the dansylation proce-

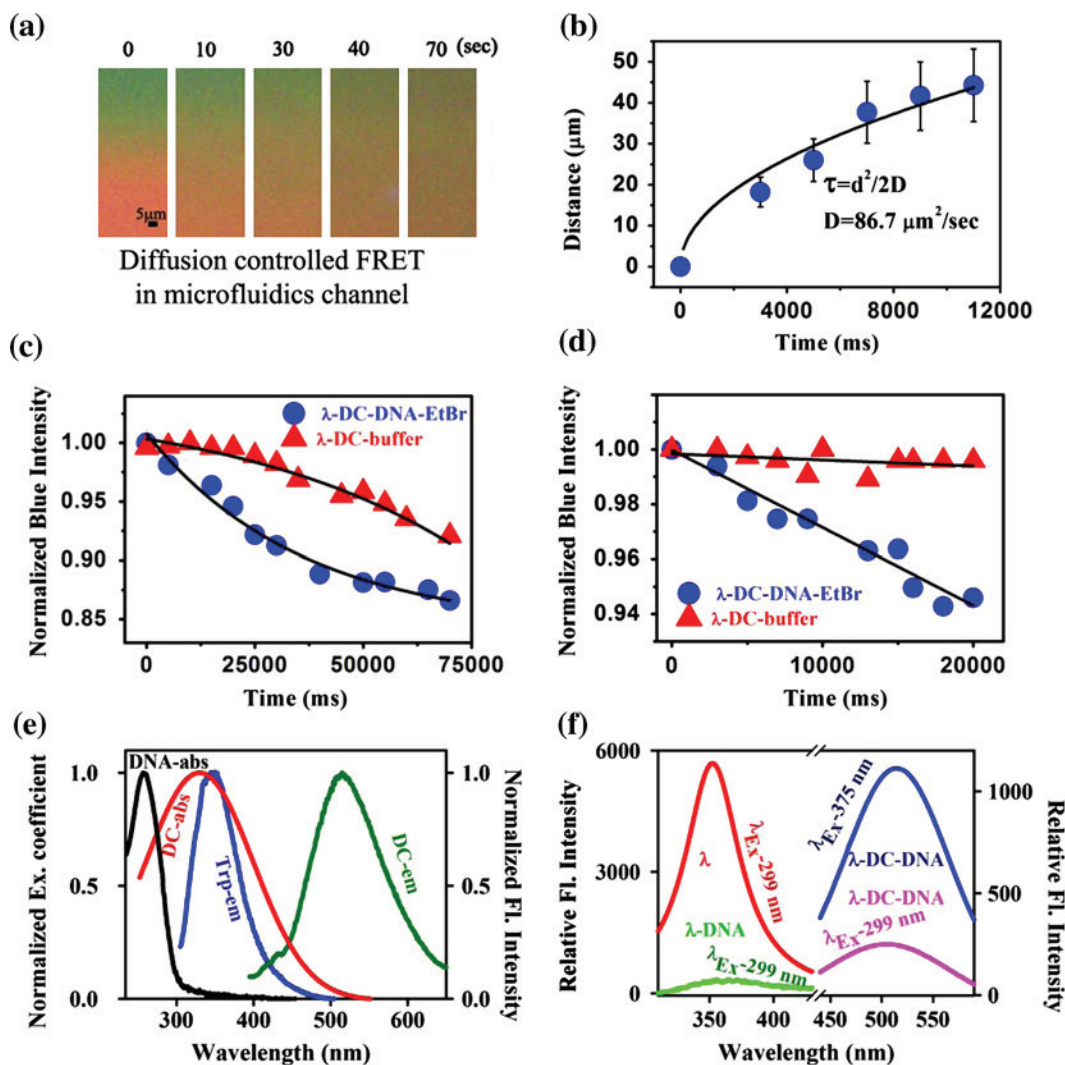


Figure 2. Diffusion-controlled FRET in microfluidics channel. (a) Fluorescence microscopic images of dansylated  $\lambda$ -repressor- $O_{R1}$  DNA-EtBr complex at a fixed position of microfluidics channel in different time window. (b) Diffusion of the biomolecule (dansylated  $\lambda$ -repressor) under study. (c) Change in normalized blue intensity of dansylated  $\lambda$ -repressor in buffer ( $\lambda$ -DC-buffer; red) and dansylated  $\lambda$ -repressor- $O_{R1}$  DNA-EtBr complex ( $\lambda$ -DC-DNA-EtBr; blue) with time (up to 70 s). The excitation and emission wavelengths were 365 and 515 nm, respectively. (d) Same as described in caption (c) within a smaller time window (20 s). (e) The steady-state absorption spectra of DNA (DNA-abs; black), Dansyl (DC-abs; red), and emission spectra of tryptophan in  $\lambda$ -repressor (Trp-em; blue), dansyl bound to  $\lambda$ -repressor (DC-em; green) are shown. (f) Steady-state fluorescence spectra of tryptophan in  $\lambda$ -repressor ( $\lambda$ ; red) and in  $\lambda$ -repressor- $O_{R1}$  DNA complex ( $\lambda$ -DNA; green). Systems were excited at 299 nm. Steady-state fluorescence spectra of dansyl in dansylated  $\lambda$ -repressor- $O_{R1}$  DNA complex at excitation wavelength 375 nm ( $\lambda$ -DC-DNA; blue) and 299 nm ( $\lambda$ -DC-DNA; pink) are shown.

ture are given in supplementary material. Briefly, labeling of  $\lambda$ -repressor with dansyl chloride was done according to a previous work (Banik, Mandal, Bhattacharyya, & Roy, 1993). Labeled repressor concentration was determined by bicinchoninic acid assay using bovine serum albumin as a standard. The incorporation ratio of dansyl was found to be  $1.1 \pm 0.2$  (Banik et al., 1993). It has to be noted that the modification procedure essentially attaches dansyl chromophore to the lysine residue of the protein (Hsieh & Matthews, 1985) and lysine with

higher solvent-accessible surface area may have higher possibility for the modification.

Figure 2(a) shows the diffusion-controlled complexation of  $\lambda$ -repressor with operator DNA ( $O_{R1}$ ) with increasing time. The snapshots represent the interfacial region of the two reagent streams (dansyl-modified repressor in the upper side of the channel, EtBr-bound operator DNA in the lower side of the channel) during the diffusion-controlled complexation. The green and red fluorescence represent the emission of dansyl-modified



$\lambda$ -repressor and EtBr bound to DNA, inside the microfluidics channel, respectively. As the emission of EtBr (red) has a tail in the green region, we have monitored the blue light intensity as an indicator of the protein-bound dansyl fluorescence. The decrease in the blue fluorescence intensity with time (up to 70 s) is an indication of energy transfer from dansyl in the protein to DNA-bound EtBr (Figure 2(c)). The control experiment is done using dansylated  $\lambda$ -repressor and phosphate buffer as reference to consider the dilution effect on the fluorescence intensity of dansyl-modified  $\lambda$ -repressor upon mixing. Within a smaller time window (Figure 2(d)), the blue fluorescence intensity for the reference system changes insignificantly in comparison with the dansylated  $\lambda$ -repressor–DNA–EtBr complex, which confirms the occurrence of FRET as mentioned above. Moreover, for the system under investigation, the diffusion of the biomolecules with increasing time is also monitored and represented in Figure 2(b). The diffusion coefficient is calculated to be  $86.7 \mu\text{m}^2 \text{s}^{-1}$ . From the obtained diffusion coefficient, the radius of the biological molecule under investigation is estimated to be  $\sim 30 \text{ \AA}$ , which stunningly resembles the radius of the  $\lambda$ -repressor protein.

The steady-state absorption spectra of DNA, dansylated  $\lambda$ -repressor, and the emission spectra of  $\lambda$ -repressor before (excitation 299 nm) and after (excitation 375 nm) dansylation, are shown in Figure 2(e). The emission spectrum of tryptophan in  $\lambda$ -repressor shows a distinct peak at 350 nm upon excitation at 299 nm, which becomes significantly quenched after binding with operator DNA as evident from Figure 2(f). The decrease in steady-state fluorescence of tryptophan in  $\lambda$ -repressor upon binding to operator DNA reflects PET from tryptophan to DNA, as already reported for some other different biological systems in the literature (Milligan et al., 2003; Wagenknecht, Stemp, & Barton, 2000). The dansyl-modified  $\lambda$ -repressor–DNA complex shows an emission maxima at 515 nm (excitation at 375 nm), which is found to be significantly quenched when excited at 299 nm, as shown in Figure 2(f). It has to be noted that the optical density at both the excitation wavelengths (299 and 375 nm) is similar (Figure 2(e)). The reduced fluorescence intensity of dansyl in dansyl-modified  $\lambda$ -repressor–DNA complex at 299 nm excitation compared to that at 375 nm excitation wavelength could also be an indicative of ET reaction from dansyl to operator DNA at the excitation wavelength of 299 nm.

The  $\lambda$ -repressor monomer contains three tryptophan residues at position W129, W142, and W230. The latter two are in the C-terminal domain while the first one is in the hinge region. The tryptophan fluorescence transients within  $\lambda$ -repressor (at three detected wavelengths – 330, 350, and 380 nm) in the absence of the operator DNA depict similar decay profiles revealing similar

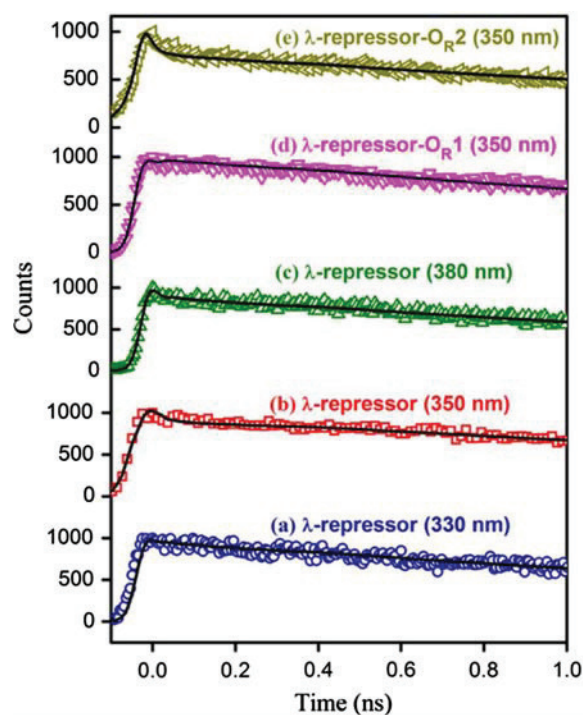


Figure 3. The picosecond-resolved fluorescence transients of tryptophan residues in  $\lambda$ -repressor detected at (a) 330 nm ( $\lambda$ -repressor (330 nm); blue), (b) 350 nm ( $\lambda$ -repressor (350 nm); red), and (c) 380 nm ( $\lambda$ -repressor (380 nm); green). The picosecond-resolved fluorescence transients of tryptophan residues within  $\lambda$ -repressor in the presence of (d)  $O_{R1}$  DNA, detected at 350 nm ( $\lambda$ -repressor– $O_{R1}$  (350 nm); pink) and (e)  $O_{R2}$  DNA, detected at 350 nm ( $\lambda$ -repressor– $O_{R2}$  (350 nm); dark yellow).

environments around the tryptophan residues (depicted in Figure 3), which is evident from the insignificant change in the lifetime of tryptophan at these wavelengths (supplementary Table SI). It is also evident from the figure that the nature of the fluorescence decay profile of tryptophan in  $\lambda$ -repressor (detected at 350 nm) changes insignificantly in the presence of operators DNA ( $O_{R1}$  and  $O_{R2}$ ) revealing an insignificant possibility of perturbation of tryptophan emission transients detected at 350 nm, due to other non-emissive processes. In Figure 4(a), the fluorescence transients of tryptophan residues within  $\lambda$ -repressor in the presence and absence of  $O_{R1}$  DNA (at various wavelengths) are shown. However, in the presence of  $O_{R1}$  DNA, although the fluorescence transient of tryptophan at 350 nm remains essentially unaltered (Figure 3), the decay profiles at 330 and 380 nm become significantly faster (Figure 4(a)), revealing a faster time constant  $\sim 20$  ps.

The corresponding time constants are tabulated in supplementary Table SI. The observation clearly reveals a non-radiative channel for the buried (Vivian & Callis, 2001) (emitting at the blue end of the tryptophan emission spectrum, e.g. 330 nm) and solvent-exposed

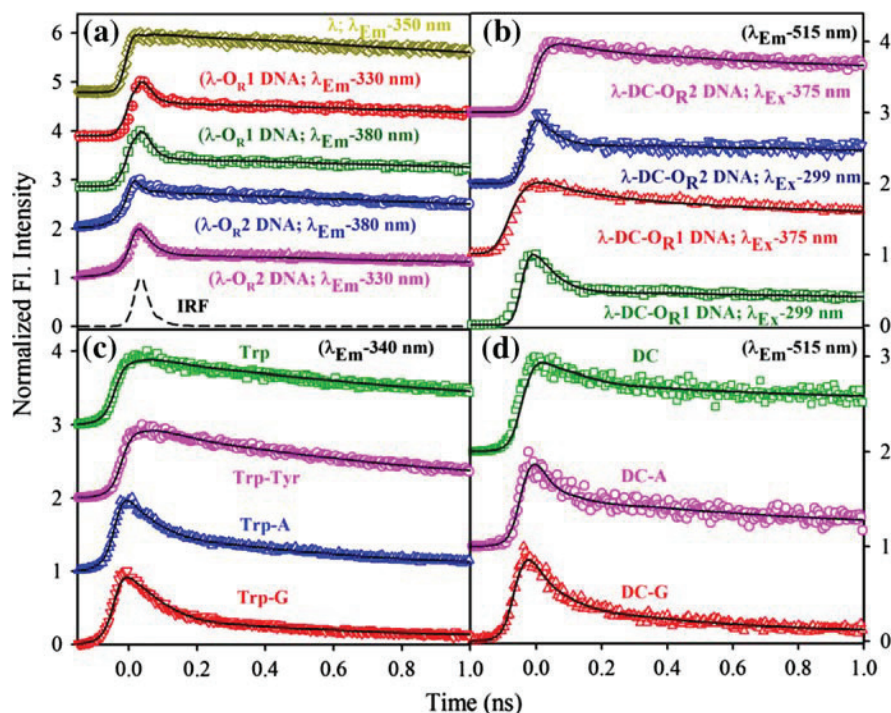
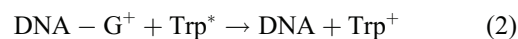
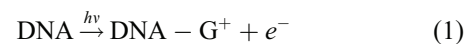


Figure 4. (a) The picosecond-resolved fluorescence transients of tryptophan in  $\lambda$ -repressor in the absence of DNA detected at 350 nm ( $\lambda$ ;  $\lambda_{Em}$ -350 nm; dark yellow), in the presence of O<sub>R1</sub> DNA detected at 330 nm ( $\lambda$ -O<sub>R1</sub> DNA;  $\lambda_{Em}$ -330 nm; red) and 380 nm ( $\lambda$ -O<sub>R1</sub> DNA;  $\lambda_{Em}$ -380 nm; green) and in the presence of O<sub>R2</sub> DNA detected at 330 nm ( $\lambda$ -O<sub>R2</sub> DNA;  $\lambda_{Em}$ -330 nm; pink) and 380 nm ( $\lambda$ -O<sub>R2</sub> DNA;  $\lambda_{Em}$ -380 nm; blue). Excitation wavelength is 299 nm. The black dotted line represents the Instrument Response Function. (b) Fluorescence transients of dansyl in  $\lambda$ -repressor-O<sub>R1</sub> DNA complex, excited at 375 nm ( $\lambda$ -DC-O<sub>R1</sub> DNA;  $\lambda_{Ex}$ -375 nm; red) and at 299 nm ( $\lambda$ -DC-O<sub>R1</sub> DNA;  $\lambda_{Ex}$ -299 nm; green). Fluorescence transients of dansyl in  $\lambda$ -repressor-O<sub>R2</sub> DNA complex, excited at 375 nm ( $\lambda$ -DC-O<sub>R2</sub> DNA;  $\lambda_{Ex}$ -375 nm; pink) and at 299 nm ( $\lambda$ -DC-O<sub>R2</sub> DNA;  $\lambda_{Ex}$ -299 nm; blue). Emission wavelength is 515 nm ( $\lambda_{Em}$ -515 nm). (c) Fluorescence transients of tryptophan only (Trp; green) and tryptophan in the presence of adenine (Trp-A; blue), in the presence of guanine (Trp-G; red), and in the presence of *N*-acetyl tyr (Trp-Tyr; pink). Emission and excitation wavelengths are 340 nm and 299 nm, respectively. (d) Fluorescence transients of dansyl (DC; green) and dansyl in the presence of adenine (DC-A; pink) and in the presence of guanine (DC-G; red) are shown. Emission and excitation wavelengths are 515 and 299 nm. The baselines are shifted for clarity.

(Petrich, Longworth, & Fleming, 1987) (emitting at the red end of the tryptophan emission spectrum, e.g. 380 nm) tryptophan residues in  $\lambda$ -repressor-O<sub>R1</sub> DNA complex. It has to be noted that tryptophan can be considered as buried (in non-polar environments) if the fluorescence maximum is near or less than 330 nm and water exposed (in polar environments) if fluorescence peak is longer than 330 nm (Petrich et al., 1987). The fluorescence transients of tryptophan residues within  $\lambda$ -repressor in the presence and absence of O<sub>R2</sub> DNA detected at various wavelengths are also depicted in Figure 4(a). Although the fluorescence transient of tryptophan at 350 nm, upon addition of O<sub>R2</sub> DNA, remains unaltered (Figure 3), the decay profile of tryptophan at 330 nm becomes faster, revealing an ultrafast time constant of  $\sim$ 20 ps. We assign the ultrafast non-radiative decay of the tryptophan residues to be due to PET. In our excitation wavelength (299 nm), the possibility of formation of guanyl radicals in the DNA due to the removal of a single electron from guanine cannot be ruled out

(Milligan et al., 2003). Therefore, tryptophan (reduction potential of its single electron oxidation product at pH 7 is +1.03 V) that has a lower oxidation potential than guanine (reduction potential of guanosine, +1.29 V) can act as electron donor or hole acceptor retrieving the native state of guanine from its radical cation (Milligan et al., 2003) (Figure 1). Therefore, the excited-state reaction scheme can be given as below:



We have also estimated the ET rate  $k_{ET}$  for different systems in the following way (Robel, Kuno, & Kamat, 2007):

$$k_{ET} = \frac{1}{\tau_{\text{Trp-O}_R1\text{DNA}} \text{ or } \tau_{\text{Trp-O}_R2\text{DNA}}} - \frac{1}{\tau_{\text{Trp}}} \quad (3)$$

where  $\tau_{\text{Trp}}$ ,  $\tau_{\text{Trp-O}_R1\text{DNA}}$  and  $\tau_{\text{Trp-O}_R2\text{DNA}}$  are the average lifetime of tryptophan in  $\lambda$ -repressor, in  $\lambda$ -repressor- $\text{O}_R1$  DNA complex, and in  $\lambda$ -repressor- $\text{O}_R2$  DNA complex, respectively.

The ET rate ( $k_{\text{ET}}$ ) from tryptophan to  $\text{O}_R1$  DNA at 330 and 380 nm is found to be  $1.81 \times 10^9$  and  $2.4 \times 10^9 \text{ s}^{-1}$ , respectively. The ET rate ( $k_{\text{ET}}$ ) from tryptophan to  $\text{O}_R2$  DNA at 330 nm is found to be  $1.3 \times 10^9 \text{ s}^{-1}$ . It has to be noted that the tryptophan residues are about 30 Å away from the DNA surface (estimating the distance, using X-ray crystal structure of  $\lambda$ -repressor-operator DNA complex in VIEWER LITE software (Power Macintosh, Molecular Simulations Inc.)). In that case, the tryptophan residues may contribute to the process of long-range ET through space involving solvent, peptide bridge, or ion pairing to the operator DNA located at the N-terminal domain of the protein (Isied et al., 1992). The long-range ET rates reportedly vary from ultrafast ( $10^{10} \text{ s}^{-1}$ ) to very slow time scale ( $10^3 \text{ s}^{-1}$ ) depending on the distance as well as the system under study (Isied et al., 1992). The long-range ET rates observed in our experiment are found to be well within the rates reported in existing literature.

The structural dissimilarity between the  $\text{O}_R1$  and  $\text{O}_R2$  DNA-bound  $\lambda$ -repressors is distinctly evident from our observation. For repressor- $\text{O}_R1$  DNA complex, both the tryptophan residues (water exposed and buried) are participating equally in the ET reaction. In contrast, for the repressor- $\text{O}_R2$  DNA complex, the buried tryptophan residues are responsible for the ET reaction, whereas the rate of ET from the solvent-exposed tryptophan is significantly less  $9.8 \times 10^7 \text{ s}^{-1}$ . The observation can be correlated with the dynamical flexibility of the protein upon binding with  $\text{O}_R1$  DNA compared to that with  $\text{O}_R2$  DNA (Mondol et al., 2012). It has to be noted that the flexibility in the C-terminal domain of the protein upon DNA binding is reflected in the ET reactions in the protein-DNA complexes as most of the tryptophan residues reside in the C-terminal domain. We have also used a dansyl probe, which is located near the C-terminal region of the protein to monitor the effect of conformational dynamics on the ET rate from dansyl to DNA. It is also known that upon complexation with operator DNA, the N-terminal domain of the protein becomes frozen, while the C-terminal domain shows flexibility (Saha et al., 1992) of different degree. In this regard, ET dynamics from the dansyl to operator DNA has been studied. In principle, dansyl can also act as electron donor or hole acceptor retrieving the native state of guanine from its radical cation (Figure 1) as the oxidation potential of *N*-ethyl dansylamide (0.94 V), a derivative of dansyl, is lower than that of guanine (Guy et al., 2007). The ET dynamics of dansyl in the protein upon complexation with  $\text{O}_R1$  and  $\text{O}_R2$  DNA is evident from the faster fluorescence transients depicted in Figure 4(b). ET rate is

found to be similar for both dansyl-modified repressor- $\text{O}_R1/\text{O}_R2$  DNA complex ( $1.2 \times 10^8$  and  $1.0 \times 10^8 \text{ s}^{-1}$  for repressor- $\text{O}_R1/\text{O}_R2$  DNA complex, respectively). This may be due to the fact that the different conformations of the dansyl chromophore as a consequence of dynamical flexibility of the protein bound to operator DNA have similar ET efficiency to the DNA.

At this juncture, it has to be mentioned here that tyrosine in the protein may also act as potential electron donor (Butler, Land, Prütz, & Swallow, 1982; Prütz et al., 1982) and conformational or dynamical change in the protein upon DNA binding may also facilitate ET from the tyrosine to tryptophan, leading to the fluorescence quenching of the latter residue. The reduction potential of tryptophan (for single electron oxidation product at pH 7; +1.03 V) is greater than the reduction potential of tyrosine (for the single electron oxidation product at pH 7; +0.93 V, Milligan et al., 2003). In this regard, some control experiments have been performed with free DNA bases (guanine and adenine), amino acids (tryptophan and *N*-acetyl tyrosinamide), and dansyl amide in thin films. The molecular structures of adenine, guanine, tryptophan, and *N*-acetyl tyrosinamide are represented in the lower panel of Figure 1. In the Figure 4 (c), the fluorescence transients of tryptophan in thin film in the absence and in the presence of adenine and guanine are shown. It is evident from the figure that the temporal decay of tryptophan in the presence of adenine and guanine upon excitation at 299 nm becomes significantly faster, apparently is an indicative of PET from tryptophan to both adenine and guanine (supplementary Table SII). The ET rates ( $k_{\text{ET}}$ ) from tryptophan to guanine and adenine in our experimental condition are found to be  $3.0 \times 10^9$  and  $3.5 \times 10^9 \text{ s}^{-1}$ , respectively. The observed ET rates are similar to that observed in the protein-DNA complex as discussed above. Figure 4(c) also shows that the fluorescence decay of tryptophan is relatively less affected in the presence of *N*-acetyl tyrosinamide (Tyr), revealing ET rate constant of  $3 \times 10^8 \text{ s}^{-1}$ , which is far off from the ET rates observed in the protein-DNA complex in our present study. Figure 4(d) reveals the fluorescence transients of dansyl in the absence and in the presence of adenine and guanine upon excitation at 299 nm. The fluorescence decay of dansyl detected at 515 nm is also significantly quenched upon addition of adenine and guanine. The quenching in the time-resolved emission of dansyl signifies the occurrence of PET from dansyl to adenine and guanine. The ET rate ( $k_{\text{ET}}$ ) from dansyl to guanine and adenine (radical or cation) upon 299 nm excitation is estimated to be  $2.6 \times 10^9$  and  $1.5 \times 10^9 \text{ s}^{-1}$ , respectively. The ET rates are faster than that in the protein-DNA complex as discussed above. In contrast, the dansyl chromophore in the presence of guanine and adenine with excitation of 375 nm shows insignificant fluorescence quenching. We



have also investigated the ET reaction between dansyl and Tyr. However, insignificant change in the lifetime of dansyl in the presence of Tyr rules out the possibility of ET from dansyl to Tyr or vice versa.

### Conclusion

In summary, we have explored the effect of protein conformational dynamics on the rate of ET. We have demonstrated that the flexibility of the C-terminal domain of  $\lambda$ -repressor protein upon binding to OR1 DNA is reflected by similar kind of ET dynamics for most of the tryptophan residues. For repressor-OR2 complex, the flexibility in the C-terminal domain after binding with DNA is hindered as evidenced by differential ET dynamics of the tryptophan residues resulting from a particular orientation of the C-terminal domain conformation due to the loss of dynamical flexibility. Additionally, similar ET dynamics from the dansyl to OR1 and OR2 DNA has been observed indicating insignificant influence of the dynamics of the repressor C-terminal domain on the conformation of single dansyl. One of the fascinating finding is the long-range ET process from tryptophan to guanine in the protein-DNA complex which is conferred by time-resolved fluorescence spectroscopy. In this context, our extremely significant finding is that in spite of residing  $\sim 30$  Å away from the DNA, the tryptophan residues can serve as electron donor. We demonstrate that in a protein-DNA complex, the conformation of the protein upon complexation with the DNA is extremely crucial for the flow of electron from protein to DNA moiety.

### Supplementary material

The supplementary material for this paper is available online at <http://dx.doi.org/10.1080/07391102.2012.680035>.

### Acknowledgments

S. B. thanks CSIR, India for fellowship. We are extremely grateful to Prof. Siddhartha Roy (Indian Institute of Chemical Biology, Kolkata) for allowing us to work in his laboratory and providing us with chemicals whenever we needed. We also thank Prof. Roy for his valuable suggestions and encouragement during the entire course of the studies. We are extremely thankful to Abhishek Mazumder (Indian Institute of Chemical Biology, Kolkata) for helping us to isolate and purify the protein. We thank DST for financial grant (SR/SO/BB-15/2007).

### References

Augustyn, K.E., Merino, E.J., & Barton, J.K. (2007). A role for DNA-mediated charge transport in regulating p53: Oxidation of the DNA-bound protein from a distance. *Proceedings of the National Academy of Sciences of the United States of America*, 104, 18907–18912.

- Banik, U., Mandal, N.C., Bhattacharyya, B., & Roy, S. (1993). A fluorescence anisotropy study of tetramer-dimer equilibrium of lambda repressor and its implication for function. *Journal of Biological Chemistry*, 268, 3938–3943.
- Banik, U., Saha, R., Mandal, N.C., Bhattacharyya, B., & Roy, S. (1992). Multiphasic denaturation of the  $\lambda$ -repressor by urea and its implications for the repressor structure. *European Journal of Biochemistry*, 206, 15–21.
- Batabyal, S., Rakshit, S., Kar, S., & Pal, S.K. (2012). An improved microfluidics approach for monitoring real-time interaction profiles of ultrafast molecular recognition. *Review of Scientific Instruments*. <http://dx.doi.org/10.1063/1.4704839>.
- Becker, D., & Sevilla, M.D. (1993). The chemical consequences of radiation-damage to DNA. *Advances in Radiation Biology*, 17, 121–180.
- Benson, N., Adams, C., & Youderian, P. (1994). Genetic selection for mutations that impair the co-operative binding of lambda repressor. *Molecular Microbiology*, 11, 567–579.
- Butchosa, C., Simon, S., & Voityuk, A.A. (2010). Electron transfer from aromatic amino acids to guanine and adenine radical cations in pi stacked and T-shaped complexes. *Organic & Biomolecular Chemistry*, 8, 1870–1875.
- Butler, J., Land, E.J., Prütz, W.A., & Swallow, A.J. (1982). Charge transfer between tryptophan and tyrosine in proteins. *Biochimica et Biophysica Acta*, 705, 150–162.
- Candeias, L.P., & Steenken, S. (1993). Electron-Transfer in di(deoxy)nucleoside phosphates in aqueous solution: Rapid migration of oxidative damage (Via adenine) to guanine. *Journal of the American Chemical Society*, 115, 2437–2440.
- Chohan, K.K., Jones, M., Grossmann, J.G., Frerman, F.E., Scrutton, N.S., & Sutcliffe, M.J. (2001). Protein dynamics enhance electronic coupling in electron transfer complexes. *Journal of Biological Chemistry*, 276, 34142–34147.
- Colson, A.O., Besler, B., Close, D.M., & Sevilla, M.D. (1992). Ab initio molecular orbital calculations of DNA bases and their radical ions in various protonation states: Evidence for proton transfer in GC base pair radical anions. *Journal of Physical Chemistry*, 96, 661–668.
- Deb, S., Bandyopadhyay, S., & Roy, S. (2000). DNA sequence dependent and independent conformational changes in multipartite operator recognition by  $\lambda$ -repressor. *Biochemistry*, 39, 3377–3383.
- Gomez-Fernandez, J.C., Goni, F.M., Bach, D., Restall, C.J., & Chapman, D. (1980). Protein-lipid interaction: Biophysical studies of  $(Ca^{2+} + Mg^{2+})$ -ATPase reconstituted systems. *Biochimica et Biophysica Acta*, 598, 502–516.
- Guy, J., Caron, K., Dufresne, S., Michnick, S.W., Skene, W.G., & Keillor, J.W. (2007). Convergent preparation and photophysical characterization of dimaleimide dansyl fluorogens: Elucidation of the maleimide fluorescence quenching mechanism. *Journal of the American Chemical Society*, 129, 11969–11977.
- Hochschild, A., & Ptashne, M. (1986). Cooperative binding of  $\lambda$  repressors to sites separated by integral turns of the DNA helix. *Cell*, 44, 681–687.
- Hsieh, W.T., & Matthews, K.S. (1985). Lactose repressor protein modified with dansyl chloride: Activity effects and fluorescence properties. *Biochemistry*, 24, 3043–3049.
- Isied, S.S., Ogawa, M.Y., & Wishart, J.F. (1992). Peptide-mediated intramolecular electron transfer: Long-range distance dependence. *Chemical Reviews*, 92, 381–394.



- Jones, M., Talfournier, F., Bobrov, A., Grossmann, J.G., Vekshin, N., Sutcliffe, M.J., & Scrutton, N.S. (2002). Electron transfer and conformational change in complexes of trimethylamine dehydrogenase and electron transferring flavoprotein. *Journal of Biological Chemistry*, *277*, 8457–8465.
- Kelley, S.O., & Barton, J.K. (1998). Radical migration through the DNA helix: Chemistry at a distance. *Metal Ions in Biological Systems*, *26*, 211–249.
- Lee, P.E., Demple, B., & Barton, J.K. (2009). DNA-mediated redox signaling for transcriptional activation of SoxR. *Proceedings of the National Academy of Sciences of the United States of America*, *106*, 13164–13168.
- Meijsing, S.H., Pufall, M.A., So, A.Y., Bates, D.L., Chen, L., & Yamamoto, K.R. (2009). DNA binding site sequence directs glucocorticoid receptor structure and activity. *Science*, *324*, 407–410.
- Milligan, J.R., Aguilera, J.A., Ly, A., Tran, N.Q., Hoang, O., & Ward, J.F. (2003). Repair of oxidative DNA damage by amino acids. *Nucleic Acids Research*, *31*, 6258–6263.
- Mondol, T., Batabyal, S., Mazumder, A., Roy, S., & Pal, S.K. (2012). Recognition of different DNA sequences by a DNA-binding protein alters protein dynamics differentially. *FEBS Letters*, *586*, 258–262.
- Mondol, T., Batabyal, S., & Pal, S.K. (2012). Interaction of an antituberculosis drug with nano-sized cationic micelle: Förster resonance energy transfer from dansyl to rifampicin in the microenvironment. *Photochemistry and Photobiology*, *88*, 328–335.
- Nada, T., & Terazima, M. (2003). A novel method for study of protein folding kinetics by monitoring diffusion coefficient in time domain. *Biophysical Journal*, *85*, 1876–1881.
- Ozturk, S., Hassan, Y.A., & Ugaz, V.M. (2010). Interfacial complexation explains anomalous diffusion in nanofluids. *Nano Letters*, *10*, 665–671.
- Petrich, J.W., Longworth, J.W., & Fleming, G.R. (1987). Internal motion and electron transfer in proteins: A picosecond fluorescence study of three homologous azurins. *Biochemistry*, *26*, 2711–2722.
- Prütz, W.A., Siebert, F., Butler, J., Land, E.J., Menez, A., & Montenay-Garestier, T. (1982). Charge transfer in peptides: Intramolecular radical transformations involving methionine, tryptophan and tyrosine. *Biochimica et Biophysica Acta*, *705*, 139–149.
- Ptashne, M. (1992). *A genetic switch: Phage  $\lambda$  and higher organisms*. Boston, MA: Cell Press.
- Ridge, J.P., Fyfe, P.K., McAuley, K.E., van Brederode, M.E., Robert, B., van Grondelle, R., ... Jones, M.R. (2000). An examination of how structural changes can affect the rate of electron transfer in a mutated bacterial photoreaction centre. *Biochemical Journal*, *351*, 567–578.
- Robel, I., Kuno, M., & Kamat, P.V. (2007). Size-dependent electron injection from excited CdSe quantum dots into TiO<sub>2</sub> nanoparticles. *Journal of the American Chemical Society*, *129*, 4136–4137.
- Saha, R., Banik, U., Bandopadhyay, S., Mandal, N.C., Bhattacharyya, B., & Roy, S. (1992). An operator-induced conformational change in the C-terminal domain of the  $\lambda$  repressor. *Journal of Biological Chemistry*, *267*, 5862–5867.
- Schulten, K., & Tesch, M. (1991). Coupling of protein motion to electron transfer: Molecular dynamics and stochastic quantum mechanics study of photosynthetic reaction centers. *Chemical Physics*, *158*, 421–446.
- Vivian, J.T., & Callis, P.R. (2001). Mechanisms of tryptophan fluorescence shifts in proteins. *Biophysical Journal*, *80*, 2093–2109.
- Wagenknecht, H.A., Stemp, E.D.A., & Barton, J.K. (1999). Evidence of electron transfer from peptides to DNA: Oxidation of DNA-bound tryptophan using the flash-quench technique. *Journal of the American Chemical Society*, *122*, 1–7.
- Wagenknecht, H.A., Stemp, E.D.A., & Barton, J.K. (2000). DNA-bound peptide radicals generated through DNA-mediated electron transport. *Biochemistry*, *39*, 5483–5491.
- WebLab ViewerLite 3.1 for Power Macintosh, Molecular Simulations Inc.